Effects mediated by the α7 nicotinic acetylcholine receptor on cell proliferation and migration in rat adipose-derived stem cells

Marta Pernarella,[1]* Roberta Piovesana,[1,2]* Carlo Matera,[3] Alessandro Faroni,[2] Mario Fiore,[4] Luciana Dini,[1] Adam J. Reid,[2,5] Clelia Dallanoce,[3] Ada Maria Tata[1,6]

[1]Department of Biology and Biotechnologies "Charles Darwin", Sapienza University of Rome, Italy
[2]Blond McIndoe Laboratories, Division of Cell Matrix Biology and Regenerative Medicine, University of Manchester, UK
[3]Department of Pharmaceutical Sciences, Medicinal Chemistry Section "Pietro Pratesi", University of Milan, Italy
[4]Institute of Molecular Biology and Pathology-CNR, Rome, Italy
[5]Department of Plastic Surgery and Burns, Wythenshawe Hospital, University of Manchester, UK
[6]Research Centre of Neurobiology "Daniel Bovet", Sapienza University of Rome, Italy

*These authors equally contributed to this paper

ABSTRACT

Adipose-derived stem cells (ASCs) are an attractive source for regenerative medicine as they can be easily isolated, rapidly expandable in culture and show excellent *in vitro* differentiation potential. Acetylcholine (ACh), one of the main neurotransmitters in central and peripheral nervous systems, plays key roles in the control of several physiological processes also in non-neural tissues. As demonstrated in our previous studies, ACh can contribute to the rat ASCs physiology, negatively modulating ASCs proliferation and migration *via* M2 muscarinic receptor (mAChR) activation. In the present work we show that rat ASCs also express α7 nicotinic receptors (nAChRs). In particular, we have investigated the effects mediated by the selective activation of α7 nAChRs, which causes a reduction of ASC proliferation without affecting cell survival and morphology, and significantly promotes cell migration *via* upregulation of the CXCR4 expression. Interestingly, the activation of the α7 nAChR also upregulates the expression of M2 mAChR protein, indicating a cooperation between muscarinic and nicotinic receptors in the inhibition of ASC proliferation.

Key words: Acetylcholine; adipose-derived stem cells; alpha7 nicotinic receptor; proliferation; migration.

Introduction

Mesenchymal stem cells (MSCs) are the most common cell population used in the biological research area and regenerative medicine, considering the lack of teratoma formation and ethical issue about their harvest.[1-3] MSCs derive from the mesoderm layer that during embryogenesis originates different tissues; in the adult, they can be found in different perivascular niches, in bone marrow and adipose tissue. MSCs are an attractive tool for the clinical therapy given their easy *in vitro* expansion, their ability to differentiate into a variety of tissues producing trophic factors and cytokines and their high immunoregulatory capability.[4-7] Bone marrow cell-based therapy is probably the most successful; the safe and controlled stem cell-based therapy has been widely proposed and is potentially useful in the regenerative medicine.[8] In addition to the well-characterised MSC population from bone-marrow (BM-MSCs), MSCs are found in other tissues as adipose tissue, peripheral blood, umbilical cord blood and foetal tissue.[2] Among all the different MSCs, those derived from adipose tissue are among the most attractive in terms of therapeutic potential.[9]

Adipose tissue is composed of adipocytes, pre-adipocytes and a heterogeneous stromal cells population called stromal vascular fraction (SVF), that contains microvascular endothelial cells, blood cells, fibroblasts, smooth muscle and stem cells.[9,10] A liposuction-extracted fat is rich in resident stem cells and over 50% of non-fat cells present stem cell markers.[11] SVF population, composed of plastic-adhering cells, can be easily isolated through a mechanical and enzymatic digestion with collagenase, followed by centrifugation to remove the floating adipocytes.[9,10] As stated by the International Fat Applied Technology Society, the adopted name for the isolated, plastic-adherent, multipotent cell population is adipose-derived stem cells (ASCs).[9,10] ASCs share some features with BM-MSCs, such as extensive self-renewal ability, multipotential differentiative capability (*e.g.*, bone, fat, cartilage and muscle) and the lack of immunogenicity in autologous ASCs transplantation, allowing to bypass the use of immunosuppressive drugs.[1,9,10,12-14] Although ASCs are similar to BM-MSCs, ASCs extraction provides a 100-fold higher number of successfully isolated stem cells compared to the BM-MSC harvest.[15] In addition, ASCs are easier to culture for longer periods and show faster growth rates,[16] making this population a quite interesting tool for regenerative medicine.[17] Moreover, in humans, ASCs can be easily isolated by conventional liposuction, a less invasive procedure compared with the painful bone marrow techniques.[16,18]

ASCs exhibit excellent regenerative qualities; for example, when exposed to a hypoxic environment, they express angiogenic factors, such as vascular endothelial growth factor-1 (VEGF), hepatocyte growth factor (HGF) and transforming growth factor beta (TGF-β),[19] promoting new blood vessels sprouting. In peripheral nerve injury environment, ASCs are also able to secrete NGF and BDNF, enhancing neuronal survival.[20] Interestingly, in regenerative medicine, as described for BM-MSCs, ASCs can be differentiated into non-mesenchymal pathways under appropriate *in vitro* conditions, as Schwann-like phenotype,[18,21] skeletal[10] and cardiac[9,10] myocytes and pancreatic-like cells,[22] opening up new opportunities in cell replacement strategies[18,23] and a debate within the regenerative medicine community on the impact of MSC trans-differentiation as opposed to other cell lineages usually derived from different germ layers.[23] ASCs can work as a 'secretome', releasing growth factors in the extracellular matrix with a high impact on the various organs and systems.[24] Additional anti-apoptotic, anti-oxidant and anti-inflammatory properties found for ASCs further highlight their potential in regenerative medicine.[25,26]

The non-neuronal functions of the cholinergic system are largely documented, among them the involvement in the regulation of physiology of glial cells,[27,28] immune cells[29,30] and stem cells.[31,32] MSCs express choline acetyltransferase (ChAT), acetylcholinesterase (AChE); moreover, nAChR subunits and metabotropic mAChR subtypes were detected in different mesenchymal cell types.[32-34] As previously demonstrated, M2 mAChR activation negatively modulates ASC proliferation and migration.[32] Although the expression of nAChR, and in particular α7 receptor, has been reported in ASCs,[34] the functional role of this subtype has been poorly investigated so far. The α7 nAChR is a homomeric channel expressed in several areas of the central (CNS) and peripheral (PNS) nervous systems[35] as well as in other non-neuronal tissues.[36-39] In the present study, we investigated the role of the α7 nicotinic receptors in rat ASC proliferation and migration and demonstrated that their selective activation promotes ASC migration and arrests cell proliferation.

Materials and Methods

Statements for animal use

All the experiments requiring animals were performed within the Biological Services Facilities (BSF) at the University of Manchester, in accordance with the UK Animals (Scientific Procedures) Act, 1986. Following terminal anaesthesia with CO_2 and cervical dislocation (Schedule 1), tissues were harvested from the animals and processed as required to obtain the cell cultures.

Adipose-derived stem cells harvesting and culture

ASCs were harvested as previously reported;[32,40] ASCs were isolated from adult male (3 months) Sprague-Dawley rats. Fat pads were dissected and minced using a sterile razor blade. After, tissue was enzymatically digested for 1 h at 37°C using 0.15% (w/v) collagenase type I (Invitrogen, Manchester, UK). A 100 μm filter was used to remove the undissociated tissue. The solution was centrifugated at 1200 rpm for 10 min and the SVF obtained. The stromal cell pellet was plated in 75 cm² cell culture flasks in stem cell growth medium consisting in minimum essential medium (MEM, Sigma-Aldrich, UK) supplemented with 10% (v/v) foetal bovine serum (FBS, LabTech, Uckfield, UK), 1% (v/v) Penicillin/Streptomycin (Sigma-Aldrich, UK) and 1% (v/v) Glutamine (Sigma-Aldrich, UK). The cultures were maintained at sub-confluent levels in a 37°C incubator with 5% CO_2 and passaged with trypsin/EDTA (Sigma-Aldrich, UK) when required.

Cell treatments

The compound 3-methoxy-1-oxa-2,7-diaza-7,10-ethanospiro-dec-2-ene sesquifumarate (ICH3) was used to selectively activate the α7 nAChR.[41-44] ICH3 was used at the final concentration of 10 μM. α-Bungarotoxin (Tocris Bioscience, Bristol, UK), an α7 nicotinic receptor antagonist, was used at final concentration of 100 nM and it was added 2 h before ICH3 treatment. The M2 muscarinic receptor selective agonist arecaidine propargyl ester hydrobromide (APE, Sigma-Aldrich, Milan, Italy) was used at the final concentration of 100 μM.[32,45] Controls were obtained maintaining the cells in normal growth medium. Technical and experimental triplicates were performed for all experiments.

RNA extraction and RT-PCR analysis

Total RNA was extracted using Tri-Reagent (Sigma-Aldrich, UK). RNA concentration and purity were detected using the NanoDrop Lite Spectrophotometer (Thermo, Dreieich, Germany). One microgram of total RNA was reverse-transcribed into cDNA for 60 min at 37°C with 1 μg of random Primers (Promega, Italy) and 200 U of Moloney Murine Leukemia Virus (M-MLV) reverse

transcriptase (Promega, Italy). The sequences of the primers used are reported in Table 1. Glyceraldehyde-3-phospate dehydrogenase (GAPDH) was used as housekeeping gene. The densitometric analyses of the RT-PCR were performed by ImageJ imaging software (NIH, Bethesda, MD, USA).

Western blot

Cells were collected using Trypsin and centrifuged for 10 min at 1000 rpm and the whole-cells lysates were resuspended and extracted in Lysis buffer (10 mM TrisEDTA, 0.5% NP40, 150 mM NaCl) supplemented with protease inhibitors cocktail (Sigma-Aldrich, UK). Lysates were sonicated for 15 seconds, incubated for 30 min on ice and then centrifuged for 20 min at 14,000 rpm at 4°C. Protein concentration was determined using BCA Protein Assay Kit (Thermo Scientific, Waltham, MA, USA), according to the manufacturer's protocol. Sample buffer (4×) was added to the protein sample, heated for 5 min at 100°C, loaded onto a 12% SDS polyacrylamide gel and run at 100 V using running buffer (0.25 M Tris, 2.4 M Glycine, 0.035 M SDS). SDS-PAGE gels were transferred onto PVDF membranes (Polyvinylidene fluoride, Merck Millipore, Darmstadt, Germany) at 200 mA in transfer buffer (20 mM Tris; 150 mM glycine, 10% [v/v] methanol) for 2 h at 4°C. Membranes were blocked for 30 min in 5% of non-fat dry milk (Sigma-Aldrich, Italy) in Tris-buffer saline (TBS) containing 0.1% Tween-20, and then incubated, at 4°C overnight, with the antibodies previously diluted in the blocking solution. Primary antibodies used were: rabbit anti-α7 antibody (dilution 1:500, Bioss, MA, USA, bs-1049R), mouse anti-M2 antibody (dilution 1:800, NovusBio, CO, USA, NB120-2805), rabbit anti-CXCR4 (dilution 1:300, NovusBio, CO, USA, AB_10001320), rabbit anti-Cyclin D1 (1:100, Santa Cruz Biotechnology, CA, USA), mouse anti-β-actin (1:2000; Immunological Sciences, Rome, Italy; AB-24008). After overnight incubation, membranes were washed three times with PBS-0.1% Tween-20 buffer and then incubated for 1 h at room temperature (RT) with secondary antibody: anti-rabbit horseradish peroxidase (1:10000, Promega, Italy) or anti-mouse horseradish peroxidase (1:10000, Immunological Sciences). Membranes were exposed to ECL chemiluminescence reagent (Immunological Science) for signal detection. The bands were detected by exposition to Chemidoc (Molecular Imager ChemiDoc XRS + System with Image Lab Software, Bio-Rad, CA, USA). Band intensities were quantified as optical density using ImageJ imaging software (NIH, Bethesda, MD, USA).

Immunocytochemistry

ASCs were seeded in completed medium at the density of 4x10³ on coverslips arranged in 24 well-plates. The following day, cells were treated as required by experimental plan. Then ASCs were washed three times with PBS and fixed with 4% paraformaldehyde in PBS for 20 min at RT. After three washes in PBS, cells were pre-incubated in PBS solution containing 0,1% Triton X–100, 1% bovine albumin serum (BSA) and 10% normal goat serum (NGS) for 45 min at RT. Cells were then incubated with a polyclonal rabbit anti-α7 antibody (dilution 1:100; Bioss, bs-1049R) at 4 °C overnight. The next day, after three washes in PBS,

cells were incubated with Alexa-488-conjugated goat anti-rabbit (IgG diluted 1:200 in PBS + 0.1% Triton X-100 + 1% NGS; Immunological Sciences) for 2 h at RT. After three washes in PBS, the cells were mounted with Anti-Fade Mounting Medium with 4',6-diamidino-2-phenylindole (DAPI, Immunological Science).

The images were acquired with a Zeiss fluorescence microscope, using a 20x objective through the Axion Vision program (Zeiss, Oberkochen, Germany).

Proliferation assay-MTT assay

ASCs were seeded on 24-well plate at the density of 25 x 10³ cells/well. After 24 h of plating, cells were treated with 10 µM ICH3 and incubated at different times, up to 96 h. Cell growth was assessed by a colorimetric assay based on 3-(4,5-dimethylthiazol-2-y1)-2,5-diphenyltetrazolium bromide (MTT, Sigma-Aldrich, St. Louis, MO, USA) metabolization. For each well, the OD at 570 nm was measured by GloMax Multi Detection System (Promega, Madison, WI, USA). Cells maintained in different experimental condition were photographed by a phase contrast microscope (Axiovert, Zeiss).

Rescue of cell proliferation

To assess whether the ICH3-induced reduction of cell proliferation was reversible, a recovery analysis was set up. Cells were seeded in 60 mm diameter plates at a cell density of 60 x 10³ cells/dish. The day after seeding, the cells were treated with 10 µM ICH3 and maintained in culture for 48 h. After two days, complete medium containing ICH3 was removed from the culture medium; the cells were washed once with sterile PBS, and fresh complete media added for 48 h. Then the cells were collected by trypsinization and counted.

Flow cytometry assay

The cells were plated on 90 mm diameter dishes at a density of 200 x 10³ cells/dish. The day after plating, cells were treated with 10 µM ICH3 for 48 h. At the end of the treatment, cells were incubated for 90 min with 45 µM bromodeoxyuridine (final concentration) (BrdU, Sigma-Aldrich, UK), collected by trypsinization, centrifuged for 10 minutes at 1000 rpm and then fixed in methanol/PBS 1:1 (v/v). To identify cells in S phase, DNA content and BrdU incorporation were determined in simultaneous analysis by staining with propidium iodide (PI) and anti-BrdU respectively. Partial DNA denaturation was performed by incubating the cells in 3 N HCl for 45 min, followed by neutralization with 0.1 M sodium tetraborate. Samples were then incubated with monoclonal mouse anti-BrdU (1:50 v/v; Dako, Santa Clara, CA, USA; RRID: AB_10013660) for 60 min at RT, washed twice with 0.5% Tween-20 in PBS and incubated for 45 min with anti-mouse Alexa 488-conjugated (1:600) (Promega Italia, Milan, Italy). After washing samples with PBS plus 0.5% Tween-20, cells were stained with 10 µg/ml PI for 15 min at RT. Flow cytometry analysis was performed with a flow cytometer Coulter Epics XL with 488 nm wavelength excitation and 10⁴ events were collected for each sample. Bi-parametric (DNA content versus BrdU content) analyses were performed using WinMDI 2.9 software.

Table 1. Primer sequences used in semiquantitative RT-PCR analysis

Gene	Forward	Reverse
GAPDH	5'-TGGCATTGTGGAAGGGCTCATGAC-3'	5'-ATGCCAGTGAGCTTCCCGTTCAGC-3'
α7	5'-AACCATGCGCCGTAGGACA-3'	5'-CTCAGCCACAAGCAGCATGAA-3'
M2	5'-GCTCCAATGATTCGACGTCA-3'	5'-CGAAGTGGAAACTGTTGTTTTCAT-3'
CXCR4	5' GCCATGGCTGACTGGTACTT 3'	5' GATGAAGGCCAGGATGAGAA 3'
CyclinD1	5 -CCCTCTGCACGCACTTGAAG-3	5 -GCGAGCCATGCTTAAGACTGA-3

Wound healing

Cell migration was evaluated through wound healing assay; 300×10^3 cells were plated in a 60 mm diameter plate. Cells were maintained in complete medium until semi-confluence was reached. The experimental conditions, each of which made in triplicate, were control, 10 μM ICH3 and 10 μM ICH3 plus 100 nM αBTX. The day of wound healing test, cells were pre-treated with the antagonist (αBTX) for 2 h before the agonist and then they were also pre-treated with ICH3 for 1 h before scratch, as required in the experimental plan. After pre-treatment, wound was generated with p200 tip. The cells were photographed at time 0 h and after 6 h from the scratch using a 20x magnification objective. The space between two fronts at time 0 (t0) and 6 h (t6) was measured. The two values were subtracted, obtaining the covered space by the cells in the experimental time chosen. After 6 h, cells were fixed with 4% paraformaldehyde (PFA) in PBS (Sigma-Aldrich, UK), permealized for 15 min with 0.2% (v/v) Triton-X100 in PBS (Sigma-Aldrich, UK) and stained for 20 min at RT with Alexa 488-conjugated phalloidin (1:40, Life Technologies, UK) diluted in PBS +1% (w/v) BSA. Images were obtained using a fluorescence microscope (Zeiss) and processed with ImageJ imaging software (NIH, Bethesda, MD, USA).

Statistical analysis

Data analyses were performed with GraphPad Prism 6.0 (GraphPad Software Inc, La Jolla, CA). Data were presented as the mean ± SEM. Student's *t*-test was used for the analyses of RT-PCR and western blot whereas one-way ANOVA test followed by Bonferroni's post-test was used to evaluate statistical significance within the different samples in proliferation analyses, Cyclin D1 Western blot, FACS analysis and migration assays. A value of $p<0.05$ was considered statistically significant: $p<0.05$ (*), $p<0.01$ (**), $p<0.001$ (***) and $p<0.0001$ (****).

Results

Characterization of the α7 nicotinic receptor in ASCs

ASCs are positive for different markers including CD29, CD44, and CD90. Previously, the characterization of stemness markers to confirm the stemness nature of ASCs cultures was performed.[32] The α7 nAChR expression was analysed in ASCs by RT-PCR and Western blot analysis, which allowed to detect expression of both α7 transcript (Figure 1A) and protein, respectively (Figure 1B). We evaluated whether the activation of the α7 subtype could

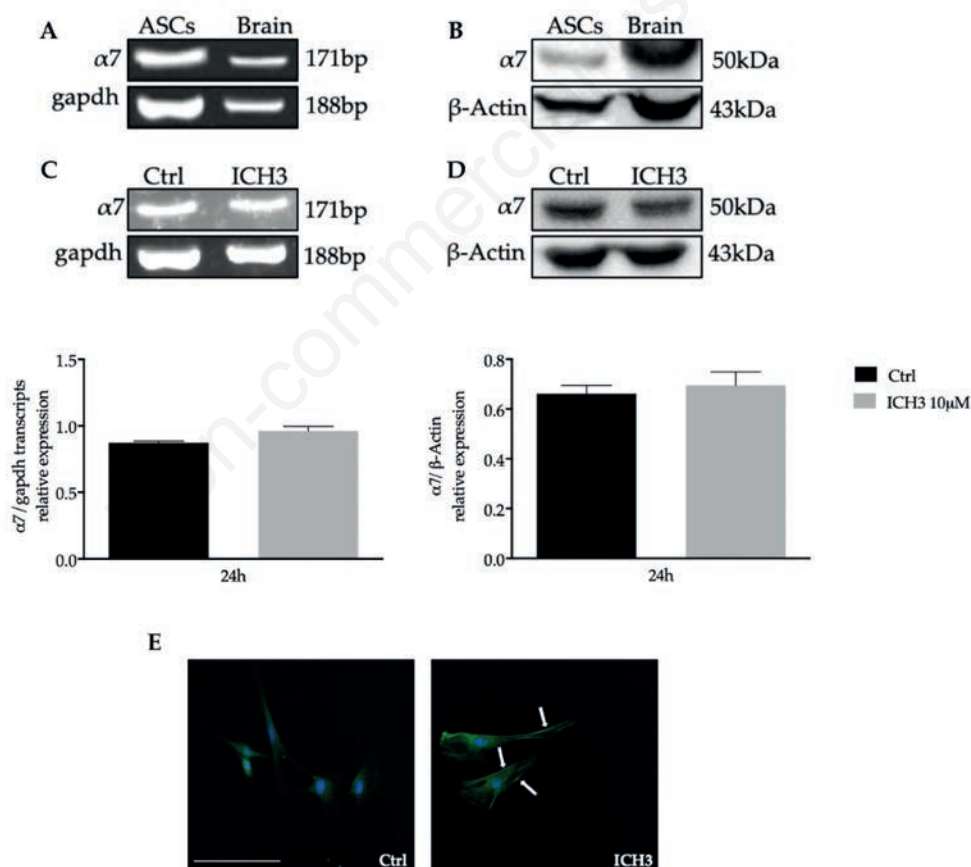**Figure 1.** α7 nicotinic receptor expression. ASCs express α7 receptor as transcript (RT-PCR) (A) and protein (Western blot) (B); rat brain was used as positive control. RT-PCR (C) and Western blot (D) analysis of the α7 receptor transcript in the absence or presence of 10 μM ICH3; the cells treated for 24 h do not show any particular variation of transcript and protein levels. GAPDH was used as housekeeping gene, whereas β-actin as reference protein; data are represented as mean ± SEM of three independent experiments. E) Immunocytochemistry analysis for α7 in ASCs following treatment with ICH3; the arrows indicate the receptor localization at cell membrane level; scale bar: 50 μm.

induce an autocrine regulation of its expression in ASCs. To this aim, ASCs were treated with the selective agonist 3-methoxy-1-oxa-2,7-diaza-7,10-ethanospiro-dec-2-ene sesquifumarate (ICH3)[41-44] at the final concentration of 10 μM. Treatment with the agonist did not induce a significant modulation of the expression of the α7 receptor both at the transcriptional and protein level, as demonstrated by the RT-PCR and Western blot analysis, respectively (Figure 1 C,D). The expression of this receptor was further analysed through immunocytochemistry. Although this approach did not allow a quantitative analysis, the level of receptor expression resulted unchanged, while receptor distribution appeared different. Indeed, in the untreated cells the staining was mainly cytoplasmic, whereas a marked staining at plasma membrane was observed after treatment with ICH3 (Figure 1E).

Activation of the α7 receptor inhibits ASC proliferation

Using MTT analysis, we found that the activation of the α7 nAChR by the selective agonist ICH3 negatively regulated ASC proliferation. ASCs treated with 10 μM ICH3 up to 96 h showed a reduction of cell growth, which was already significant after 24 h of treatment (Figure 2A). As shown in Figure 2B, the phase-contrast images indicated that, in presence of ICH3, the number of ASCs was significantly reduced. No evidence of dead floating cells was observed. To confirm that this effect is mediated by the selective activation of the α7 receptor, cells were pre-treated with the antagonist α-Bungarotoxin (100 nM) and then with ICH3. The number of cells counted after this treatment indicated that αBTX was able to counteract the effects of ICH3 (Figure 2C).
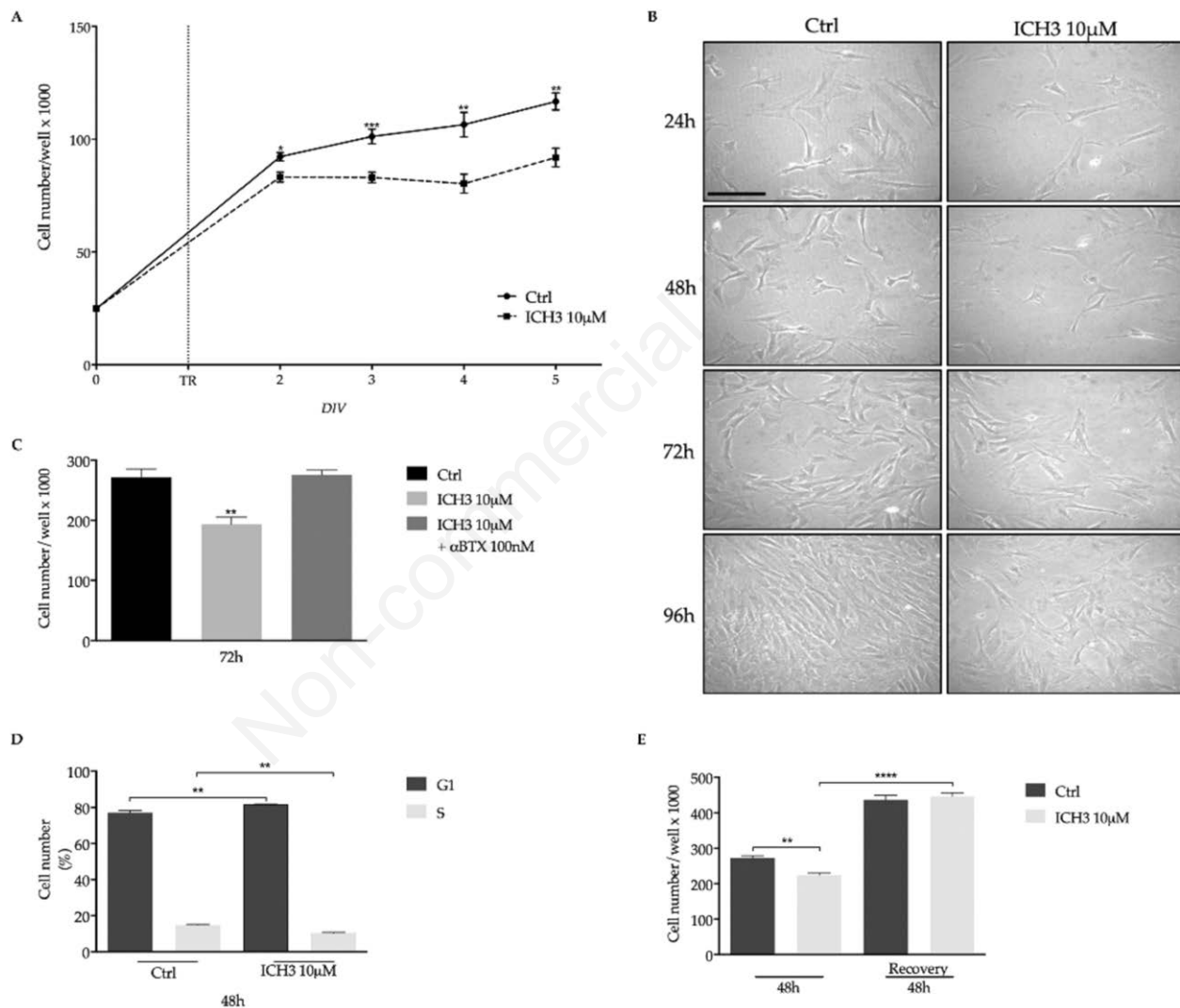

Figure 2. The activation of α7 receptor causes a reversible decrease of cell proliferation. A) Analysis of cell growth by MTT assay showed a decrease of cell growth in ASC cultures treated with 10 μM ICH3 (*P<0.05; **P<0.01; ***P<0.001) (DIV= day *in vitro*). B) Images show a decreased number of cells/field. The absence of floating cells is observable; scale bar: 100 μm. C) Cell counts performed after 72 h of treatment with 10 μM ICH3 in presence or absence of 100 nM αBTX, showed that the antagonist was able to counteract the ICH3-mediated reduced cell number (**P<0.01). D) Percentage of cells in G1 and S phases obtained by FACS analysis; after ICH3 treatment a significant reduction of cells in S phase and an increase in G1 phase were observed (**p<0.01). E) Recovery analysis assessed by cell count; following 10 μM ICH3 treatment for 48 h, after agonist withdrawal from the culture medium the cells were maintained in complete medium for additional 48 h. The data showed a full recovery of the cell proliferation rate (**p<0.01; Ctrl *vs* ICH3; ****p< 0.0001; ICH3 *vs* ICH3 recovery). The results are the mean ± SEM of at least three independent experiments conducted in triplicate.

To confirm the hypothesis regarding the α7 receptor's ability to control cell proliferation, we performed a FACS analysis in which ASCs were maintained in the presence or absence of 10 μM ICH3 for 48 h. As indicated in the Figure 2D, ASCs following treatment with ICH3 showed a significant reduction of the percentage of cells in S phase compared to the control condition. However, measuring the time of replication, we obtained a significant reduction of the cell proliferation rate with a replication time of 120 h (after 2 days *in vitro*) and 300 h (after 3 days *in vitro*; *data not shown*).

By considering the negative effects of α7 nAChR stimulation on cell proliferation, a recovery assay was performed to understand if ASCs were able to restore their proliferative rate after nicotinic agonist withdrawal. Cells were thus plated and treated for 48 h with 10 μM ICH3. Then, the agonist was removed, and a fresh medium was added. The cell number was assessed by cell count 48 h after the α7 agonist withdrawal. ASCs were able to rescue the normal proliferative rate condition, indicating that the treatment with the selective agonist caused a reduction of proliferative rate that can be restored after the agonist withdrawal (Figure 2E). To better characterize the decreased cell proliferation after α7 nAChRs activation, we performed the analysis of Cyclin D1 expression. The analysis of the transcript of Cyclin D1 by RT-PCR showed that the treatment with ICH3 significantly reduced its expression level (Figure 3A), whereas Western blot analysis showed a meaningful increase of protein levels following α7 nAChR activation. The increased ICH3-induced Cyclin D1 protein expression was counteracted by the α7 antagonist αBTX (Figure 3B).

α7 nicotinic receptors modulate ASC migration

To evaluate the α7 agonist effect on cell migration, the wound healing technique was used (Figure 4A). When required, αBTX was added to the culture medium 2 h before ICH3 treatment. Six hours after scratch, the distance between the two fronts was measured in the treated and untreated cells, as described in Materials and Methods. The graph shows the distance travelled by the cells in the chosen experimental time and indicates that the selective α7 receptor activation significantly increased cell migration (Figure 4B). The α7 antagonist αBTX counteracted the enhanced ICH3-induced cell migration.

Being the CXCR4 receptor a protein involved in the chemotactic activities, we investigated whether the increased migration observed could be related to a modulated expression of this chemokine receptor. The analysis of the CXCR4 protein expression showed that the α7 agonist treatment caused a significant increase of the levels of CXCR4 receptor protein, whereas we did not observe any modulation at transcriptional levels (Figure 4 C,D).

Cross-interaction between α7 nicotinic and M2 muscarinic receptors

Given the results obtained in a previous study about the M2 receptor meaningful upregulation after exposure to the M2 receptor agonist, APE,[32] we examined the putative modulation of the α7 nAChR and M2 mAChR expression upon treatment with M2 receptor agonist and ICH3. Figure 5A shows the lack of a significant modulation of the α7 receptor protein expression after treatment with the M2 receptor agonist APE. Instead, although the treatment with ICH3 did not affect the transcript level of the M2 receptor (Figure 5C), a significant increase of the M2 receptor protein level was detected (Figure 5D).

Discussion

In the present work, we confirm the cholinoceptivity of rat ASCs. They express α7 nAChRs subtype and its selective activation causes a reversible reduction of cell proliferation without affecting neither cell survival nor morphology and significantly promoting cell migration.

Adipose tissue is a complex tissue formed by different types of cells, including stem cells.[13] It is an abundant source of stem cells
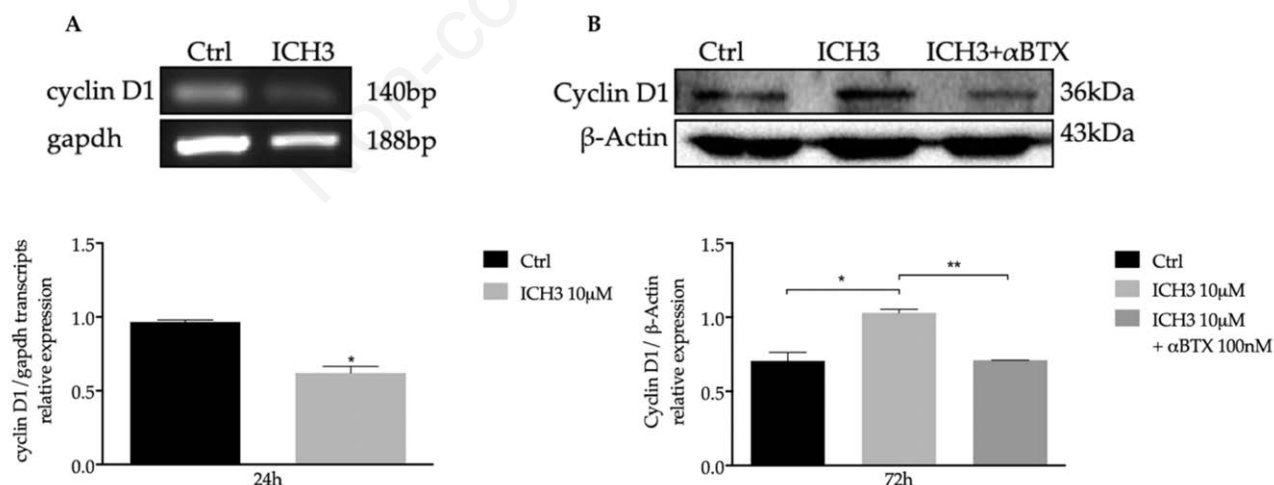

Figure 3. The selective activation of α7 receptor modulates the expression of Cyclin D1. A) RT-PCR expression analysis of Cyclin D1 in ASCs in the presence or absence of 10 μM ICH3; treatment with ICH3 caused a significant reduction in the transcript level of Cyclin D1; the graph below indicates the densitometric analysis of the bands obtained from three independent experiments, normalized with the housekeeping gene, *GAPDH* (*p<0.05). B) Western blot and densitometric analysis of the levels of Cyclin D1 protein in untreated cells (Ctrl), and cells treated with 10 μM ICH3 or 10 μM ICH3 + 100 nM α-BTX (72 h); α-BTX was added to the culture medium 2 h before ICH3 treatment; the selective activation of the α7 receptor induced a significant increase of the expression of Cyclin D1, whereas the presence of the α7 antagonist, αBTX, counteracted the effects of ICH3, resulting in an expression of Cyclin D1 comparable to that of control; β-Actin was used as the reference protein (*p<0.05; **p<0.01).

with a great trans-differentiation capability and an easier withdrawal, and these properties make this population very attractive for regenerative medicine.[12,15,18,23,46] Moreover, the role of ASCs as a secretome relevantly impacts on the homeostasis of different organs and systems.[24] Since all these features are regulated by different modulators and growth factors,[33] a full understanding of the ASC biology is far from being achieved.

In addition to its function as a neurotransmitter, ACh plays different roles in several non-neuronal tissues.[38,47-52] In a previous paper, we highlighted that ASCs respond to ACh and that the selective stimulation of M2 mAChRs negatively regulates ASC proliferation and migration, preserving ASCs in a quiescent state until the maintenance of M2 receptor activation.[32] According with the results from other authors, MSCs, and ASCs, express other cholin-

ergic receptors, such as different nicotinic subtypes,[33,34] and they are able to synthesize ACh, suggesting the existence of an autocrine and/or paracrine cholinergic circuit.[33,53] In this paper, we clearly show that rat ASCs express the α7 nAChR both as transcript and protein. Our analysis on ASCs took advantage of the application of ICH3, which was characterized as a selective orthosteric agonist of the α7 receptor subtype.[41-44] Although the selective activation with ICH3 did not modify the level of α7 receptor neither as transcript nor as protein, however a different localization, from cytoplasm to the cell membrane, was observed after exposure to ICH3 indicating that the selective stimulation contributes to export the α7 receptor on the plasma-membrane. Based on our previous data, which indicated a substantial upregulation of the M2 subtype after exposure to an M2 agonist[32], the analysis of α7
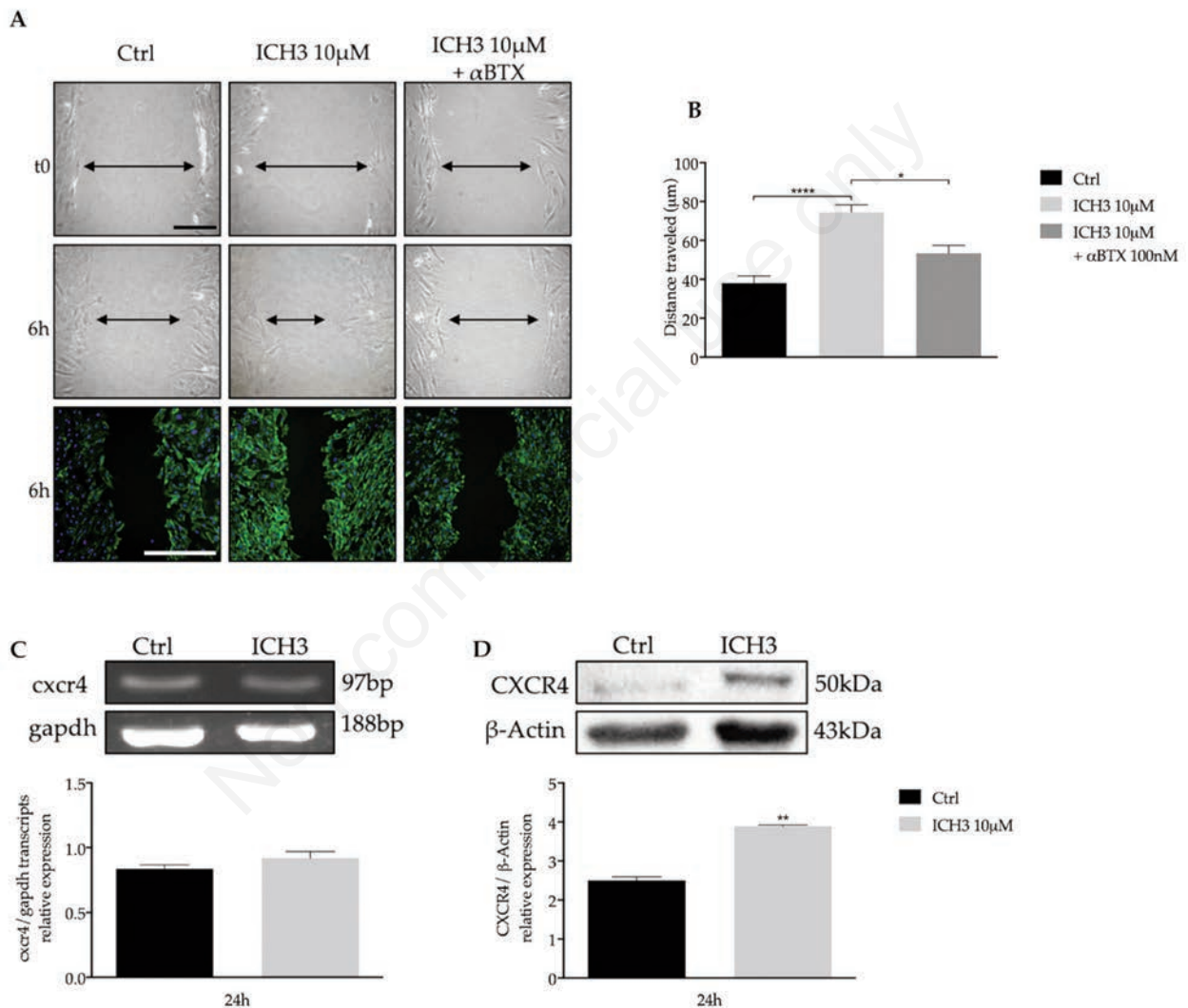

Figure 4. Analysis of ASC migration. A) The analysis of cell migration was performed by the wound healing assay; the images obtained at time 0 h (t0) corresponded to the time at which the scratch was performed, and after 6 h (t6), to analyse the width of scratch in the control and ICH3-treated cells; the distance of the gap between two fronts was measured at the two different time points; scale bar: 100 μm; the bottom panel shows the cells stained with phalloidin; scale bar: 100 μm. B) The graph shows the distance travelled by the cells (t0-t6) in the different experimental conditions; ICH3 treatment significantly increased cell migration; the data obtained are the mean ± SEM at least three independent experiments carried out in triplicate (****p<0.0001 Ctrl *vs* ICH3; *P<0.05 ICH3 *vs* ICH3+αBTX). C) RT-PCR analysis of the CXCR4 transcript after 10 μM ICH3 treatment; the graph indicates the densitometric analysis of the bands normalized against GAPDH, used as housekeeping gene; transcript level remained unchanged after ICH3 treatment. D) Western blot and densitometric analysis of CXCR4 protein in untreated (Ctrl) and treated (10 μM ICH3) cells for 24 h; β-actin was used as reference protein (**p<0.01); although ICH3 treatment did not change the expression of CXCR4 transcript, it induced a significant upregulation of the protein level; the results are the mean ± SEM of three independent experiments.

expression did not show any significant modulation after APE treatment. On the other hand, an upregulation of the M2 receptor protein was evidenced after α7 receptor stimulation, suggesting a cross-modulation in ASCs of the two different cholinergic receptor types. The nicotinic stimulation decreased cell growth up to four days after treatment without affecting cell survival, with a reduction of the percentage of cells in S phase after 48 h of treatment; this event was counteracted by the selective α7 nicotinic antagonist, αBTX. Since we did not observe floating cells, this suggest the absence of dead cells, demonstrating that the treatment used does not affect cell survival. Taking the advantage by FACS analysis data, we calculated the duplication time and found a significant increase of the time used for replication after 72 h of treatment, suggesting that the α7 receptor stimulation causes a decrease of the ASC proliferation rate rather than an arrest of their cell cycle. This result is also confirmed by the ability of the ASCs to rescue cell proliferation; in fact the reduction of cell growth was reversible and cells recovered their proliferative rate after withdrawal of the α7 agonist, similarly to what observed after M2 receptor stimulation.[32] The α7-mediated inhibition of cell proliferation detected by MTT and FACS analysis was followed by a significant downregulation of the Cyclin D1 transcript level and, in contrast, with a significant upregulation of the Cyclin D1 protein level. The two opposite effects could be explained by a temporary

block of the cells in S phase; in this condition, the increased level of the Cyclin D1 protein may be a consequence of cell accumulation and this may directly influence also the expression of the Cyclin D1 transcript. Interestingly, αBTX counteracted the modulated expression of the Cyclin D1 protein, thus validating the selectivity of the agonist and the specific involvement of the α7 receptor subtype. ACh, through M2 receptors, is also able to decrease cell growth[32] and adult stem cells and other cells in the stem niche synthetize ACh, as indicated by the expression of the related biosynthetic enzyme ChAT. Therefore, we may hypothesize that ACh, by activating receptor-dependent cholinergic pathways, is able to inhibit ASC proliferation, preserving their quiescent status and plasticity.

Cell migration is a fundamental event for stem cells, which allows their movement from the stem cell niches to reach the damaged tissue to maintain the tissue homeostasis and to modulate inflammatory and regenerative processes. Cell migration is depending on CXCL12/SDF-1-CXCR4/CXCR7 pathway.[54] In our experiments, we evidence that the α7 agonist ICH3 efficiently promotes ASC migration, with a relevant upregulation of the CXCR4 protein level. Even these positive effects mediated by the α7 receptor were counteracted by the selective antagonist αBTX. Thus, our data suggest that ACh could act as one of the factors modulating ASC migration, which is promoted or arrested *via* activation of α7

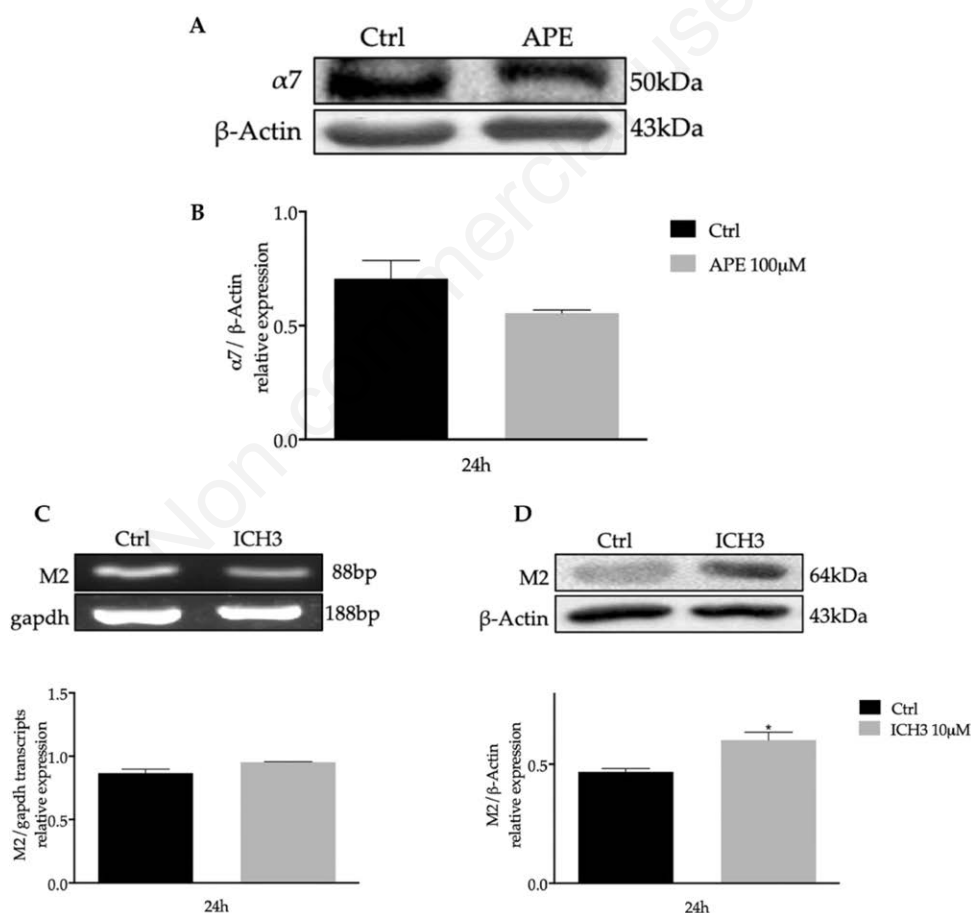**Figure 5. Cross-interaction between nicotinic and muscarinic receptors. A,B)** Protein analysis by Western blot of the α7 receptor following treatment with 100 μM APE for 24 h did not show any variation of the protein level; β-actin was used as the reference protein. **C)** RT-PCR analysis did not show any modulation of the M2 muscarinic receptor after α7 receptor stimulation; *GAPDH* was used as housekeeping gene. **D)** M2 receptor protein expression was significantly upregulated after ICH3 treatment as indicated by western blot analysis; β-actin was used as the reference protein; the analyses were carried out following the treatment with 10 μM ICH3 for 24 h; the data represented are the mean ± SEM of three independent experiments; *p<0.05.

nicotinic or M2 muscarinic receptors, respectively.

In conclusion, the results obtained in this study clearly demonstrate the role of ACh and its receptors in the modulation of ASC proliferation and migration. Although more detailed investigations are needed to fully understand how and when the different cholinergic receptors are expressed by ASCs *in vivo*, our data confirm the additional non-neuronal functions of ACh and its receptors as reported in different tissues,[38,47,48,52,55] and indicate that the cholinergic transmission, mediated by M2 and α7 receptors, may contribute to the modulation of the physiological process of ASCs.

Acknowledgements

References

1. Frith J, Genever P. Transcriptional control of mesenchymal stem cell differentiation. Transfus Med Hemother 2008;35: 216-27.
2. Bobis S, Jarocha D, Majka M. Mesenchymal stem cells: Characteristics and clinical applications. Folia Histochem Cytobiol 2006;44:215-30.
3. Rodrigues M, Griffith LG, Wells A. Growth factor regulation of proliferation and survival of multipotential stromal cells. Stem Cell Res Ther 2010;1:1-12.
4. Nakagami H, Morishita R, Maeda K, Kikuchi Y, Ogihara T, Kaneda Y. Adipose tissue-derived stromal cells as a novel option for regenerative cell therapy. J Atheroscler Thromb 2006;13:77-81.
5. Castro-Manrreza ME, Montesinos JJ. Immunoregulation by mesenchymal stem cells: Biological aspects and clinical applications. J Immunol Res 2015;2015:1-20.
6. Mishra VK, Shih H-H, Parveen F, Lenzen D, Ito E, Chan T-F, et al. Identifying the therapeutic significance of mesenchymal stem cells. Cells 2020;9:1145.
7. Jiang W, Xu J. Immune modulation by mesenchymal stem cells. Cell Prolif 2020;53:1-16.
8. Caddick J, Kingham PJ, Gardiner NJ, Wiberg M TG. Phenotypic and functional characteristics of mesenchymal stem cells differentiated along a schwann cell lineage. Glia 2006;54:840-9.
9. Gimble JM, Katz AJ, Bunnell BA. Adipose-derived stem cells for regenerative medicine. Circ Res 2007;100:1249-60.
10. Strem MS, Hicok KC, Zhu M, Wulur I, Z Alfonso, Schreiber RE, et al. Multipotential differentiation of adipose tissue-derived stem cells. Keio J Med 2005;54:132-41.
11. Ilic D, Polak JM. Stem cells in regenerative medicine: Introduction: Br Med Bull 2011;98:117-26.
12. Mizuno H, Tobita M, Uysal AC. Concise review: Adipose-derived stem cells as a novel tool for future regenerative medicine. Stem Cells 2012;804-10.
13. Qomi RT, Sheykhhasan M. Adipose-derived stromal cell in regenerative medicine: A review. World J Stem Cells 2017;9:107-17.
14. Zuk PA, Zhu M, Ashjian P, De Ugarte DA, Huang JI, Mizuno H, et al. Human adipose tissue is a source of multipotent stem cells. Mol Biol Cell 2002;13:4279-95.
15. Bunnell BA, Flaat M, Gagliardi C, Patel B, Ripoll C. Adipose-derived stem cells: Isolation, expansion and differentiation. Methods 2008;45:1-11.
16. Locke M, Windsor J, Dunbar PR. Human adipose-derived stem cells: isolation, characterization and applications in surgery. ANZ J Surg 2009;79:235-44.
17. Mazini L, Rochette L, Amine M, Malka G. Regenerative capacity of adipose derived stem cells (ADSCs), comparison with mesenchymal stem cells (MSCs). Int J Mol Sci 2019;20:2523.
18. Kingham PJ, Kalbermatten DF, Mahay D, Armstrong SJ, Wiberg M, Terenghi G. Adipose-derived stem cells differentiate into a Schwann cell phenotype and promote neurite outgrowth in vitro. Exp Neurol 2007;207:267-74.
19. Zhao L, Johnson T, Liu D. Therapeutic angiogenesis of adipose-derived stem cells for ischemic diseases. Stem Cell Res Ther 2017;8:1-9.
20. Han C, Zhang L, Song L, Liu Y, Zou W, Piao H, et al. Human adipose-derived mesenchymal stem cells: A better cell source for nervous system regeneration. Chin Med J (Engl) 2014;127:329-37.
21. Jiang L, Zhu J-K, Liu X-L, Xiang P, Hu J, Yu W-H. Differentiation of rat adipose tissue-derived stem cells into Schwann-like cells in vitro. Neuroreport 2008;19:1015-9.
22. Timper K, Seboek D, Eberhardt M, Linscheid P, Christ-Crain M, Keller U, et al. Human adipose tissue-derived mesenchymal stem cells differentiate into insulin, somatostatin, and glucagon expressing cells. Biochem Biophys Res Commun 2006;341:1135-40.
23. Kingham PJ, Reid AJ, Wiberg M. Adipose-derived stem cells for nerve repair: Hype or reality? Cells Tissues Organs 2014;200:23-30.
24. Vindigni V, Giatsidis G, Reho F, Dalla Venezia E, Mammana M, Franco B. Adipose derived stem cells: current state of the art and prospective role in regenerative medicine and tissue engineering. In: J.A. Andrade, editor. Regenerative Medicine and Tissue Engineering. InTech Open; 2013. doi: 10.5772/55924.
25. Frese L, Dijkman PE, Hoerstrup SP. Adipose tissue-derived stem cells in regenerative medicine. Transfus Med Hemotherapy 2016;43:268-74.
26. Bajek A, Gurtowska N, Olkowska J, Kazmierski L, Maj M, Drewa T. Adipose-derived stem cells as a tool in cell-based therapies. Arch Immunol Ther Exp (Warsz) 2016;64:443-54.
27. Loreti S, Vilaró MT, Visentin S, Rees H, Levey AI, Tata AM. Rat Schwann cells express M1-M4 muscarinic receptor subtypes. J Neurosci Res 2006;84:97-105.
28. Uggenti C, De Stefano ME, Costantino M, Loreti S, Pisano A, Avallone B, et al. M2 muscarinic receptor activation regulates schwann cell differentiation and myelin organization. Dev Neurobiol 2014;74:676-91.
29. Di Bari M, Di Pinto G, Reale M, Mengod G, Tata AM. Cholinergic system and neuroinflammation: implication in multiple sclerosis. Cent Nerv Syst Agents Med Chem 2016;17:1-7.
30. Reale M, Di Bari M, Di Nicola M, D'Angelo C, De Angelis F, Velluto L, et al. Nicotinic receptor activation negatively modulates pro-inflammatory cytokine production in multiple sclerosis patients. Int Immunopharmacol 2015;29:152-7.
31. Zhang H, Guo D, Wang L, Zhao Y, Cheng Y, Qiao Z. Effect of nicotine on Oct-4 and Rex-1 expression of mouse embryonic stem cells. Reprod Toxicol 2005;19:473-8.
32. Piovesana R, Melfi S, Fiore M, Magnaghi V, Tata AM. M2

muscarinic receptor activation inhibits cell proliferation and migration of rat adipose-mesenchymal stem cells. J Cell Physiol 2018;233:5348-60.

33. Hoogduijn MJ, Cheng A, Genever PG. Functional nicotinic and muscarinic receptors on mesenchymal stem cells. Stem Cells Dev 2009;18:103-12.

34. Schraufstatter IU, DiScipio RG, Khaldoyanidi SK. Alpha 7 subunit of nAChR regulates migration of human mesenchymal stem cells. J Stem Cells 2009;4:203-15.

35. De Jaco A, Bernardini L, Rosati J, Tata AM. Alpha-7 Nicotinic receptors in nervous system disorders: from function to therapeutic perspectives. Cent Nerv Syst Agents Med Chem 2016;17:1-9.

36. Wang H, Yu M, Ochani M, Amella CA. Nicotinic acetylcholine receptor a 7 subunit is an essential regulator of inflammation. Nature 2003;421:384-8.

37. De Jonge WJ, Ulloa L. The alpha7 nicotinic acetylcholine receptor as a pharmacological target for inflammation. Br J Pharmacol 2007;151:915-29.

38. Fujii T, Takada-takatori Y, Kawashima K. Basic and clinical aspects of non-neuronal acetylcholine: expression of an independent, non-neuronal cholinergic system in lymphocytes and its clinical significance in immunotherapy. J Pharmacol Sci 2008;106:186-92.

39. Gallowitsch-Puerta M, Tracey KJ. Immunologic role of the cholinergic anti-inflammatory pathway and the nicotinic acetylcholine α7 receptor. Ann N Y Acad Sci 2005;1062:209-19.

40. Piovesana R, Faroni A, Magnaghi V, Reid AJ, Tata AM. M2 receptors activation modulates cell growth, migration and differentiation of rat Schwann-like adipose-derived stem cells. Cell Death Discov 2019;5:92.

41. Dallanoce C, Magrone P, Matera C, Frigerio F, Grazioso G, De Amici M, et al. Design, synthesis, and pharmacological characterization of novel spirocyclic quinuclidinyl-Δ2-isoxazoline derivatives as potent and selective agonists of α7 nicotinic acetylcholine receptors. Chem Med Chem 2011;6:889-903.

42. Di Cesare Mannelli L, Pacini A, Matera C, Zanardelli M, Mello T, De Amici M, et al. Involvement of α7 nAChR subtype in rat oxaliplatin-induced neuropathy: Effects of selective activation. Neuropharmacology 2014;79:37-48.

43. Scabia G, Cancello R, Dallanoce C, Berger S, Matera C, Dattilo A, et al. ICH3, a selective alpha7 nicotinic acetylcholine receptor agonist, modulates adipocyte inflammation associated with obesity. J Endocrinol Invest 2020;43:983-93.

44. Matera C, Dondio G, Braida D, Ponzoni L, De Amici M, Sala M, et al. In vivo and in vitro ADMET profiling and in vivo pharmacodynamic investigations of a selective α7 nicotinic acetylcholine receptor agonist with a spirocyclic Δ 2 -isoxazoline molecular skeleton. Eur J Pharmacol 2018;820:265-73.

45. Piovesana R, Faroni A, Taggi M, Matera A, Soligo M, Canipari R, et al. Muscarinic receptors modulate Nerve Growth Factor production in rat Schwann-like adipose-derived stem cells and in Schwann cells. Sci Rep 2020;10:7159.

46. Faroni A, Mobasseri SA, Kingham PJ, Reid AJ. Peripheral nerve regeneration: Experimental strategies and future perspectives. Adv Drug Deliv Rev 2015;82:160-7.

47. Kirkpatrick CJ, Grando SA, Wessler I, Kawashima K, Meurs H. The non-neuronal cholinergic system: Basic science, therapeutic implications and new perspectives. Life Sci 2012;91:969-72.

48. Wessler IK, Kirkpatrick CJ. Non-neuronal acetylcholine involved in reproduction in mammals and honeybees. J Neurochem 2017;142:144-50.

49. Eglen RM. Muscarinic receptor subtypes in neuronal and non-neuronal cholinergic function. Auton Autacoid Pharmacol 2006;26:219-33.

50. Wessler I, Kirkpatrick CJ. Acetylcholine beyond neurons: The non-neuronal cholinergic system in humans. Br J Pharmacol 2008;154:1558-71.

51. Grando SA, Kawashima K, Kirkpatrick CJ, Kummer W, Wessler I. Recent progress in revealing the biological and medical significance of the non-neuronal cholinergic system. Int Immunopharmacol 2015;29:1-7.

52. Wessler I, Kilbinger H, Bittinger F, Unger R, Kirkpatrick CJ. The non-neuronal cholinergic system in humans: Expression, function and pathophysiology. Life Sci 2003;72:2055-61.

53. El-Habta R, Kingham PJ, Backman LJ. Adipose stem cells enhance myoblast proliferation via acetylcholine and extracellular signal-regulated kinase 1/2 signaling. Muscle Nerve 2018;57:305-11.

54. Liu M, Lei H, Dong P, Fu X, Yang Z, Yang Y, et al. Adipose-derived mesenchymal stem cells from the elderly exhibit decreased migration and differentiation abilities with senescent properties. Cell Transplant 2017;26:1505-19.

55. Wessler I, Kirkpatrick CJ, Racké K. The cholinergic "pitfall": Acetylcholine, a universal cell molecule in biological systems, including humans. Clin Exp Pharmacol Physiol 1999;26:198-